Fizika Nizkikh Temperatur, 2007, v. 33, No. 8, p. 844–848

The electromagnetic response of a superconducting ferromagnets

Grigory I. Leviev, Menachem I. Tsindlekht, Edouard B. Sonin, and Israel Felner

The Racah Institute of Physics, The Hebrew University of Jerusalem, Jerusalem 91904, Israel
E-mail: gileviev@vms.huji.ac.il

Received September 19, 2006, revised December 7, 2006

The electromagnetic response of the superconducting ferromagnets $RuSr_2Gd_{1.5}Ce_{0.5}Cu_2O_{10}$ (Ru–1222 Gd) in an ac magnetic field of finite amplitude is investigated. Taking into account weak links between granules and magnetization of the magnetic sublattice, it is shown that the response of a sample in a superconducting state with the fundamental frequency and frequency of the 3rd harmonic can be described by the nonlinear equation for the macroscopic field. Generation of the harmonic at temperatures above superconducting transition corresponds to Rayleigh`s mechanism. Using various regimes of a sample cooling, the internal magnetic field determined by the magnetic sublattice was measured. This is direct evidence of the coexistence of ferromagnetic and superconductive order parameters in high-T_c ruthenocuprates.

PACS: 74.70.Pq Ruthenates;
74.25.Nf Response to electromagnetic fields.

Keywords: electromagnetic response, superconducting ferromagnets, high-T_c ruthenocuprates.

1. Introduction

The nature of the coexistence of the long-range magnetic and superconducting order parameters is discussed intensively, since Ginzburg's work [1]. The origins of the order parameters in ferromagnetic superconductors, magnetic structure and magnetic properties of such materials are hot topic in the present time [2]. Magnetic characteristics of superconducting ferromagnets such as Ru–1222 Gd is extremely interesting [3]. Those samples exhibit a magnetic transition at T_N = 125–180 K and superconducting transition at T_c = 25–50 K ($T_N > T_c$). However experimental study of the low frequency electrodynamics is almost absent. In the present paper we study the behavior of the ceramic samples Ru–1222 Gd in the presence of dc and low-frequency magnetic fields at temperatures both above and below of the superconducting transition temperature. Our measurements [4] show that the critical current in the superconducting state is very small. It leads to the specific character of the response of the sample with respect to the ac fields. The response becomes nonlinear already at small amplitudes and then — at high enough amplitudes — the linear modes return. Experimentally in our case nonlinearity also appearers at $T_c < T < T_N$, but the mechanism in this temperature range is different as the characters of the curves are completely different. In particular, the generation of all harmonics is well described by the Rayleigh`s mechanism for ferromagnetic materials [5,6].

Once a remanent magnetization is induced above T_c those materials «remember» it even when they are cooled down to $T < T_c$, and the internal field which is created, can induce the so-called spontaneous vortex phase. The purpose of the present paper is to show how this internal field can be evaluated through the amplitude of the third harmonic generation signal.

2. Experimental details

We studied the response of a Ru–1222 Gd sample to an ac magnetic field. A ceramic sample with dimensions of $8 \times 2 \times 2$ mm was prepared by a solid-state reaction as described in Ref. 4. In all experiments described here we measured the voltage drop induced in a pickup coil, which is proportional to the time derivative of the magnetization $\mathbf{M}(t)$. Our home made experimental setup was adapted to a commercial MPMS SQUID magnetometer. An ac field $h(t)$ at a frequency of $\omega/2\pi = 1.5$ kHz and an amplitude up to the $h_0 = 3$ Oe was generated by a copper

solenoid existing inside the SQUID magnetometer. The two signals at the fundamental and at the harmonic frequencies were simultaneously recorded. The temperature, dc magnetic field, and amplitude dependencies of the fundamental and harmonic signals have been measured by the two coils method. In the present paper only the results of the first and third harmonics will be discussed.

3. Experimental results and discussion

The magnetization of a sample can be expressed by the macroscopic field inside the sample $\mathbf{B}(r,t)$ and the homogeneous ac field $\mathbf{h}(t) = \mathbf{h}_0 \cos(\omega t)$ to which the sample was exposed:

$$\mathbf{M}(t) = 1/(4\pi V)\int [\mathbf{B}(\mathbf{r},t) - \mathbf{h}(t)]\, dV = \\ = \mathbf{h}_0 \sum \chi'_n \cos(n\omega t) - \chi''_n \sin(n\omega t), \quad (1)$$

where the integration is made over a volume of the sample V and χ'_n, χ''_n are the in-phase and out-of-phase susceptibilities. Here we expand the magnetization to Fourier series [7,8]. Generally speaking χ'_n and χ''_n depend on: the temperature T, the external magnetic field H and the amplitude of the ac field h_0.

3.1. Susceptibility at $H = 0$

Figure 1 shows the zero field cooled (ZFC) temperature dependence of the in-phase magnetic susceptibility χ'_1 and the amplitude of the third harmonic $A_{3\omega} \propto |\chi'_3 - i\chi''_3|$, measured at $H = 0$.

The temperature dependence of $\chi'_1(T)$ is typical for superconducting ferromagnets [9]. This plot reveals three transitions: (i) the paramagnetic-antiferromagnetic transition at $T_N \approx 125$ K, (ii) the most pronounced transition, which corresponds to peak at $T_m \approx 78$ K, and (iii) the transition into a superconducting state at $T_c \approx 28$ K. The nature of the second transition, which is evident in both the linear and nonlinear responses, is not yet completely clear

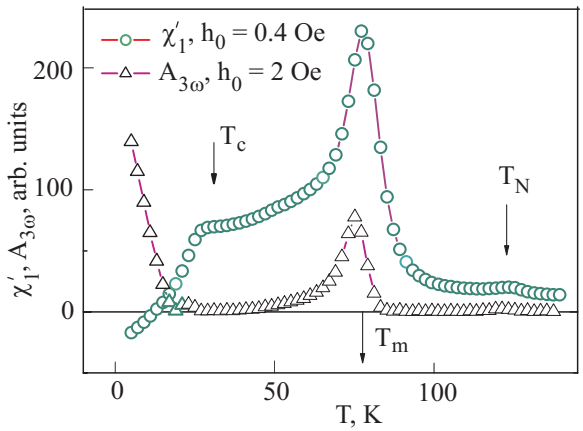

Fig. 1. Temperature dependencies of χ'_1 and $A_{3\omega}$ at $H = 0$.

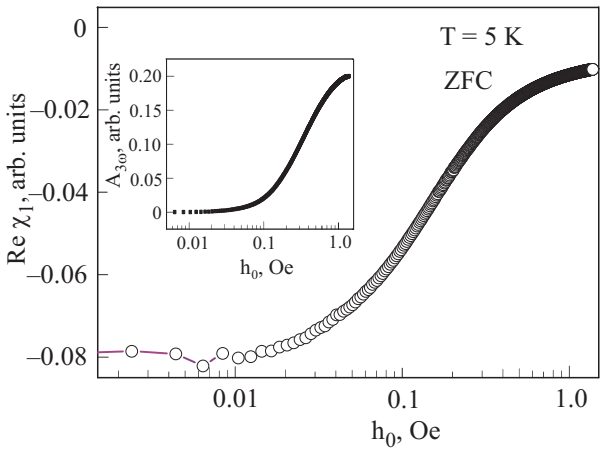

Fig. 2. Amplitude dependencies of χ'_1. Inset: amplitude dependence $A_{3\omega}$ after ZFC at $T = 5$ K.

and it is discussed elsewhere [10]. Ambiguity is connected with the magnetic phase between T_m and T_N, which is characterized by low coercivity. However, the low-temperature side near the T_m transition definitely corresponds to a weak ferromagnetic phase, and is discussed here.

The amplitude dependencies of $\chi'_1(h_0)$ and $A_{3\omega}(h_0)$ are shown on Fig. 2. The χ'_1 dependence looks like a step function. Similar behavior is observed for $A_{3\omega}(h_0)$. At $T > T_c$ $A_{3\omega}(h_0)$ is different, and its typical dependence is presented at Fig. 3.

We shall discuss the amplitude dependencies for χ_1 and $A_{3\omega}$ in a superconducting state. Let us start with the microscopic Maxwell`s equation:

$$\text{curl}\, \mathbf{h}(\mathbf{r},t) = \frac{4\pi}{c}\mathbf{j}(\mathbf{r},t), \quad (2)$$

where $\mathbf{r}$ is a radius-vector, t is time, and $\mathbf{j}$ is current density. For macroscopic values it is necessary to average both parts of this equation over a certain volume, which includes many grains. The average current density is given by

$$\langle \mathbf{j}(\mathbf{r},t) \rangle = \mathbf{j}_J + c \cdot \text{curl}\, \mathbf{M}_s + c \cdot \text{curl}\, \mathbf{M}_g . \quad (3)$$

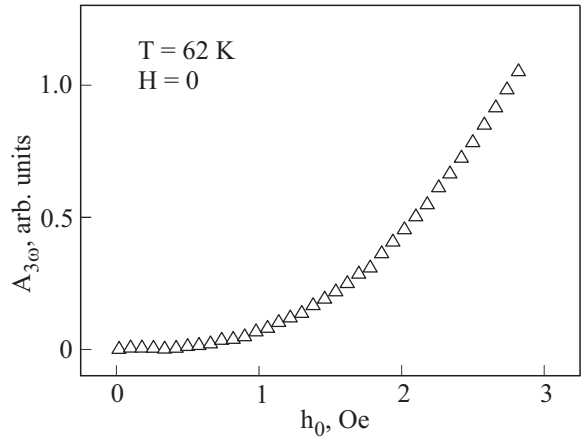

Fig. 3. Amplitude dependencies of $A_{3\omega}$ after ZFC at $T = 62$ K.

Here the average current density is the sum of the contributions from Josephson's junctions $\mathbf{j}_J$, and is proportional to the spin magnetization $\mathbf{M}_s$ and to the magnetization $\mathbf{M}_g$ caused by superconducting currents inside the grains. Using the relation $\mu \equiv 1 + 4\pi\chi_s + 4\pi\chi_g$, where μ is permeability, χ_g and χ_s are the grains and lattice susceptibilities, one obtains the macroscopic Maxwell equation:

$$\text{curl}\, \mathbf{B}(\mathbf{r},t) = \frac{4\pi\mu}{c}\, \mathbf{j}_J(\mathbf{r},t)\,. \qquad (4)$$

There is no doubt, that in granular superconductors the nonlinearity in the superconducting state is caused by weak links between grains through which Josephson's currents $\mathbf{j}_J$ flow. This current averaged over numbers of junctions can be expressed by the parameters describing the granulated media. By combining the current density expression [11,12] and Maxwell`s equation (4) we obtain the nonlinear equation for the vector potential $\mathbf{A}(\mathbf{r},t)$, which describes the behavior of a sample exposed to an ac field with finite amplitude:

$$\text{curl curl}\, \mathbf{A} = -\frac{1}{\lambda_j^2}\mathbf{A}\exp\left(-\frac{A^2}{\lambda_j^2 B_j^2}\right) - \frac{\tau}{\lambda_j^2}\frac{d\mathbf{A}}{dt}\,, \qquad (5)$$

where λ_j, B_j, τ are defined by the average parameters of the media. These parameters are: $\lambda_j^2 = c\Phi_0/(I\pi^3\rho\mu a_0^2)$, $B_j^2 = 4\Phi_0 I\rho\mu/c$, $\tau = \lambda_j^2\pi^2 a_0^2\rho\mu/(2Rc^2)$, here Φ_0 is a flux quantum, I is average current of junction, ρ is number of junctions per unit volume, a_0 is average distance between grain centers, R is the junction resistance in a resistive junction model. Parameter τ represents a characteristic time of the problem. The vector potential $\mathbf{A}$ permits one to define the magnetization of the sample $\mathbf{M}$ and the susceptibilities of the sample.

Let us consider: (a) the sample as an infinite slab of thickness d located at $-d/2 \le x \le d/2$, (b) the external ac field $h(t)$ is along the y axis, and (c) the vector potential $\mathbf{A}$, electric field $\mathbf{E}$, a current density $\mathbf{j}_J$ are all directed to z axis. Then only derivatives over x and t of the z component of the vector potential A_z exist. (Further the index z will be omitted.) Now we obtain:

$$\frac{d^2A(x,t)}{dx^2} = \frac{1}{\lambda_j^2}A(x,t)\exp\left(-\frac{A^2(x,t)}{\lambda_j^2 B_j^2}\right) + \frac{\tau}{\lambda_j^2}\frac{dA(x,t)}{dt}\,. \qquad (6)$$

The solution of Eq. (6) for the vector potential at the fundamental frequency looks as follows:

$$A(x,t) = \frac{1}{2}[A_0(x)\exp(i\omega t) + A_0^*(x)\exp(-i\omega t)] =$$

$$= |A_0|\cos(\omega t + \theta)\,.$$

Using Fourier-transformation, one can get for the amplitude $A_0(x)$ the second order ordinary differential equation:

$$\frac{d^2A_0(x,t)}{dx^2} = \lambda_j^{-2}A_0(x)\Psi[A_0(x)] + i\omega\tau\lambda_j^{-2}A_0(x)\,. \qquad (7)$$

Function

$$\Psi(y) = \exp\left(-\frac{|y|^2}{2\lambda_j^2 B_j^2}\right)\left[I_0\left(\frac{|y|^2}{2\lambda_j^2 B_j^2}\right) - I_1\left(\frac{|y|^2}{2\lambda_j^2 B_j^2}\right)\right]$$

takes into account the nonlinearity of the media, which is connected with Josephson's currents. Here I_0 and I_1 are modified Bessel functions. At small amplitudes, Ψ approaches to 1 and this case corresponds to the linear media. For a sample inside the ac coil, it is convenient to consider a symmetric excitation. So the boundary conditions for the magnetic induction has the form: $B(t)|_{x=-d/2} = B(t)|_{x=d/2} = B_0\cos(\omega t)$. Due to the symmetry, the vector potential is equal to zero in the middle of the slab ($x = 0$). Using Eq. (6) we can obtain the expression for the vector potential at the boundary $A_0(-d/2)$:

$$\int_0^{A_0(-d/2)} 2\left[\int_{A_0(-d/2)}^{z} y\ (\Psi(y) + i\omega\tau)\, dy + B_0^2\right]^{-1/2} dz = \frac{d}{2\lambda_j}\,. \qquad (8)$$

The dependence of the complex susceptibility of a sample on the fundamental frequency χ_1 is connected to the vector potential on the boundary:

$$\chi_1 = -\frac{1}{4\pi} + \frac{2A_0(-d/2)}{4\pi d h_0}\,. \qquad (9)$$

With the limit of low and large amplitudes of excitations, Eq. (7) becomes linear and the susceptibility in these cases is

$$\chi_1 = -\frac{1}{4\pi} + \frac{\mu\lambda^*}{2\pi d}\,\text{th}\,\frac{d}{2\lambda^*}\,, \qquad (10)$$

where $\lambda^* = \lambda_j(1 + i\omega\tau)^{-1/2} \approx \lambda_j(1 - i\omega\tau/2)$ — at low amplitudes and $\lambda^* = \lambda_j(i\omega\tau)^{-1/2}$ — at large amplituded. The transition from low to the large amplitudes occurs at a field about B_j. In our experiments $B_j \approx 0.015$ Oe. The ratio γ between the real part of the susceptibility at low and high amplitudes is

$$\gamma = \frac{\chi_1'(h_0 << B_j)}{\chi_1'(h_0 >> B_j)} = \frac{-1 + 2\mu\lambda_j/d}{-1 + \mu}\,.$$

Using the experimental value of this ratio, it is possible to evaluate μ: $\mu = (\gamma - 1)/\gamma$. In our experiment we obtained $\gamma = 5$, and $\mu = 0.8$. Other parameters of the model can be evaluated as well by using the grains size a_0 and resistivity the sample ρ in a normal state. Our SEM indicates that $a_0 = (1-10)\cdot 10^{-4}$ cm, and four probe resistivity measurement at room temperature $\rho_{res} = 2.5\cdot 10^{-14}$ in Gauss

units [4]. Therefore we estimate: $\lambda_j \approx 5\cdot10^{-3} - 5\cdot10^{-2}$ cm, $\tau \approx 10^{-11} - 10^{-9}$ s, $j_c \approx 0.3 - 3$ A/cm^2, $R \approx 0.1 - 1$ Ohm.

3.2. Third harmonic generation

According to the nonlinear Eq. (5), application of an ac field at fundamental frequency causes the harmonic generation. To fit qualitatively the experimental data shown in 2 it is sufficient to substitute in the Eq. (6) the calculated field at the fundamental frequency, nonlinearly dependent on the amplitude of the excitation. The amplitude dependence of the response at $T > T_c$ in the magnetic-ordered state does not show a saturation (Fig. 3). The amplitude of 3rd harmonic exhibits square-law dependence on h_0 quite well describe by the Rayleigh mechanism [5,6]. Nonlinearity at these temperatures corresponds to oscillatory motion of the domain walls in an ac field (the hysteretic dependence of a susceptibility on a magnetic field).

3.3. Influence of an applied magnetic field

The response in the presence of a dc magnetic field depends on the prehistory and the regimes of sample cooling. The physical picture thus is complicated — there is a magnetization connected to a lattice, the sample is broken into domains, and at low temperatures magnetization of the lattice can lead to a spontaneous vortex phase [13].

We used the dependence of the amplitude of the 3rd harmonic on an external field (Fig. 4) and various cooling regimes to measure internal magnetic field in a sample, remaining after turning off the external field. The procedure of cooling of a sample which we have named internal-field cooling (IFC) is this: the sample was cooled down to T_{IFC} at an external magnetic field H_{IFC} ($T_{IFC} < T_N$). At T_{IFC}, the magnetic field was turned off and further cooled down to $T = 5$ K in zero external field. It appears that by using the IFC procedure the properties of the superconducting state were different from those measured after the regular ZFC process from temperatures above T_N. Thus, in the superconducting state, the sample senses the internal magnetic field evolved from the remanent magnetization, which was formed in the normal (not superconducting) ferromagnetic phase and then quenched on further cooling.

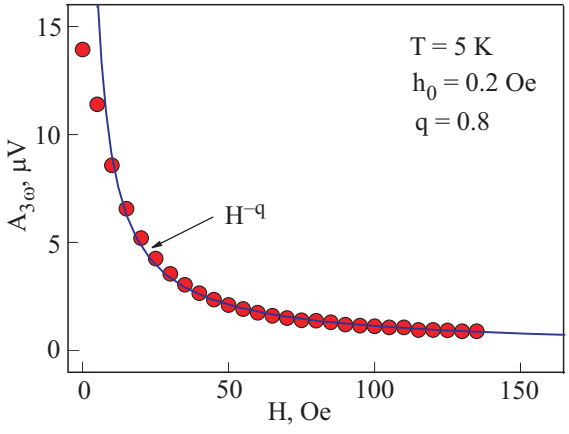

Fig. 4. Magnetic field dependence of $A_{3\omega}$ at $T = 5$ K after ZFC.

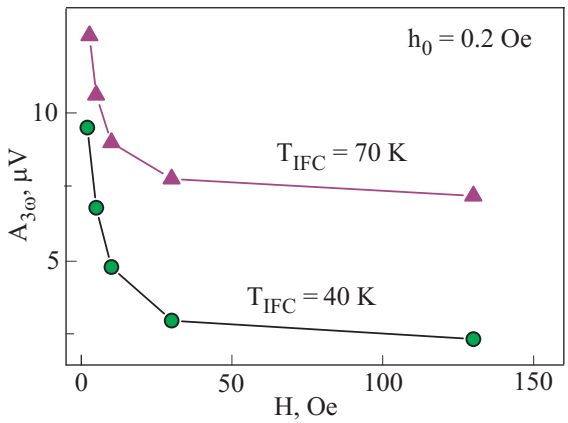

Fig. 5. $A_{3\omega}(T = 5\text{K})$ as a function of H_{IFC} for $T_{IFC} = 40$ and 70 K.

We measured the signal of the third harmonic at 5 K after the IFC procedure.

Figure 5 shows the $A_{3\omega}(H_{IFC})$ dependence for $T_{IFC} = 40$ and 70 K. It is evident that the field H_{IFC} suppresses the third harmonic as well as the external field after ZFC even though the field H_{IFC} was turned off before the superconductivity onset. The turn off H_{IFC} at $T = 40$ K affects $A_{3\omega}$ more strongly than for $T = 70$ K because the remanent magnetization in the first case is larger than for the latter.

Figure 6 presents the signal of the third harmonic $A_{3\omega}(T = 5$ K) as a function of T_{IFC} after cooling in $H_{IFC} = 30$ Oe. The signal of the third harmonic goes down for $T_{IFC} < 80$ K. This demonstrates that the suppression of the third harmonic response by the internal magnetic field takes place only if the field cooling continues down to the weakly ferromagnetic phase with essential coercivity. It is known that in idealized single-domain superconducting

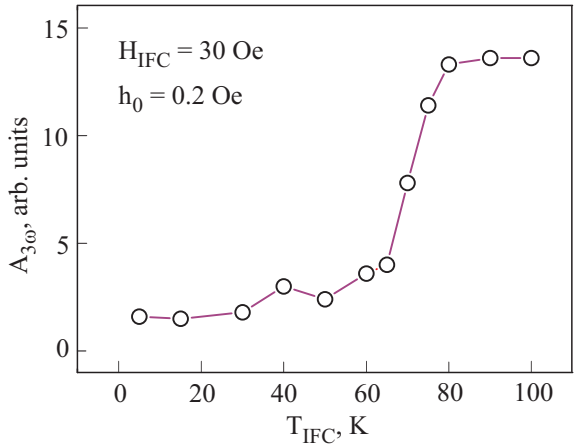

Fig. 6. Amplitude of the third harmonic $A_{3\omega}$ at $H = 0$ and $T = 5$ K versus T_{IFC}.

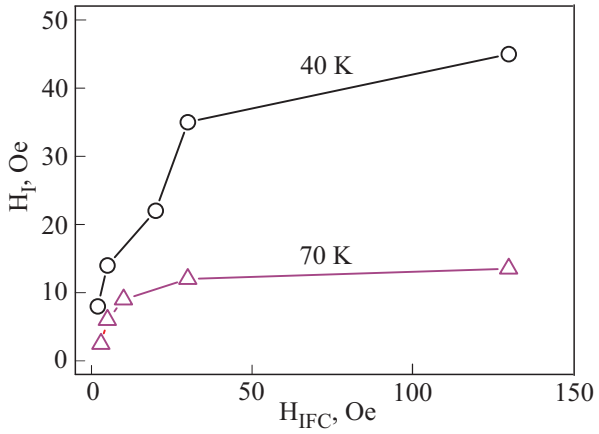

Fig. 7. Internal magnetic field versus H_{IFC} for $T_{IFC} = 40$ K and 70 K.

ferromagnets the internal magnetic field from spontaneous magnetization $4\pi M$ has the same effect on the phase diagram, i.e., on the magnetic flux penetrating into the sample, as the external field. This can be generalized in a more realistic case of a multi-domain sample with nonzero average internal field $\langle 4\pi M \rangle$. On the basis of this argument we can use the third harmonic signal versus dc magnetic field dependence as a calibration curve to estimate the magnitude of the quenched internal magnetic field H_I.

Figure 7 presents the dependence of H_I on H_{IFC}. The phenomenon revealed in our experiment is possible if the domain structure formed in the ferromagnetic phase can be quenched down to the superconducting state. On the other hand, as was noted in the pioneer paper by Ginzburg [1] and confirmed by detailed analysis in [14], superconductivity should strongly affect the equilibrium domain structure: its period should grow, and in the Meissner state any sample is a single domain in equilibrium. But in our case we deal with a nonequilibrium domain structure, which is a metastable state possible due to coercivity. The presence of the quenched internal field in the superconducting phase clearly demonstrates that the sample is in the mixed state with many vortices in the bulk. One can hardly call this state as the spontaneous vortex phase because the latter refer to the equilibrium state, but we deal with a metastable state. The nonlinear response is sensitive to the average internal field $\langle 4\pi M \rangle$. The absolute value of the average magnetization $\langle M \rangle$ is less than the saturation magnetization M, which can determine the vortex density in a single-domain sample. However, the saturation magnetization may create vortices inside domains. Since M changes its directions from a domain to a domain, we obtain the vortex tangle, which does not contribute to the average internal field $\langle 4\pi M \rangle$, studied here. This vortex tangle is expected to exist even after the ZFC process, and contributes to the initial value of the third harmonic, which was detected without external or internal magnetic field. These arguments illustrate that vorticity (magnetic flux) distribution in real especially ceramic superconducting ferromagnets can be very complicated. Genuinely zero-field cooling is practically impossible: if one cools a sample in zero external field, one cannot avoid an internal magnetic field from the spontaneous magnetization even if these fields vanish on average but still remain inside the domains.

4. Summary

In summary, our measurements of the nonlinear response unambiguously demonstrates coexistence of the superconducring and ferromagnetic order parameters in Ru-1222 samples below superconducting critical temperatures. Coexistence is manifested by the clear effect from the domain structure quenched from temperature above the superconducting critical temperatures on superconducting properties. We have shown that the nonlinear dependence of the response of a sample on a variable magnetic field manages to be understood qualitatively in all ranges of temperatures.

The work was supported by the Klatchky foundation. The authors are deeply grateful to E. Galstyan for the sample preparation and useful discussions.

1. V.L. Ginzburg, *Zh. Exp. Teor. Fiz*. **31**, 202 (1956) [*Sov. Phys. JETP* **4**, 153 (1957)].
2. V.P. Mineev, *Int. J. Mod. Phys*. **B18**, 2963 (2004); B. Lorenz and C.-W. Chu, *Nature Materials* **4**, 516 (2005); M. Faure and A.I. Buzdin, *Phys. Rev. Lett*. **94**, 187202 (2005); N.A. Logoboy and E.B. Sonin, *Phys. Rev*. **B75**, 153206 (2007).
3. D.G. Naugle, K.D.D. Rathnayaka, V.B. Krasovitsky, B.I. Belevtsev, M.P. Anatskam, G. Agnolet, and I. Felner, *J. Appl. Phy*s. **99**, 08M501 (2006).
4. I. Felner, E. Galstyn, B. Lorenz, D. Cao, Y.S. Wang, Y.Y. Xue, and C.W. Chu, *Phys. Rev*. **B67**, 134506 (2003).
5. J.W.S. Rayleigh, *Philos. Mag*. **23**, 225 (1887).
6. R.M. Bozorth, *Ferromagnetism*, D. Van Nostrand Company, Inc., NY (1951).
7. S. Shatz, A. Shaulov, and Y. Yeshurun, *Phys. Rev*. **B48**, 13871 (1993).
8. T. Ishida, and R.B. Goldfarb, *Phys. Rev*. **B41**, 8937 (1990).
9. I. Felner, U. Asaf, Y. Levi, and O. Millo *et al*., *Phys. Rev*. **B55**, R3374 (1997).
10. C.A. Cardoso, *Phys. Rev*. **B67**, 020407(R) (2003).
11. G.I. Leviev, A. Pikovsky, and D.W. Cooke, *Supercond. Sci. Technol*. **5**, 679 (1992).
12. M.V. Belodedov and V.K. Ignatjev, *Supercond. Phys. Chem. Technol*. **3**, S24 (1990).
13. E.B. Sonin and I. Felner, *Phys. Rev*. **B57**, 14000 (1998).
14. E.B. Sonin, *Phys. Rev*. **B66**, 100504 (2002).